Density Matrix and Renromalization for Classical Lattice Models

Draft Ver. 1.0 (Sep. 9. 1996)

T. Nishino[1] and K. Okunishi[2]

1 *Department of Physics, Graduate School of Science,*

Kobe University, Rokko-dai, Kobe 657, Japan

2 *Department of Physics, Graduate School of Science,*

Osaka University, Toyonaka, Osaka 560, Japan

Abstract

The density matrix renormalization group is a variational approximation method that maximizes the partition function — or minimize the ground state energy — of quantum lattice systems. The variational relation is expressed as $Z = \mathrm{Tr}\,\rho \geq \mathrm{Tr}\,(\tilde{1}\rho)$, where ρ is the density submatrix of the system, and $\tilde{1}$ is a projection operator. In this report we apply the variational relation to two-dimensional (2D) classical lattice models, where the density submatrix ρ is obtained as a product of the corner transfer matrices. The obtained renormalization group method for 2D classical lattice model, the corner transfer matrix renormalization group method, is applied to the $q = 2 \sim 5$ Potts models. With the help of the finite size scaling, critical exponents ($q = 2, 3$) and the latent heat ($q = 5$) are precisely obtained.

Address: T. Nishino, Department of Physics, Graduate School of Science,

Kobe university, Rokkodai, Kobe 657, JAPAN

Phone: +81-78-803-0541, **Fax:** +81-78-803-0722

e-mail 1: nishino@phys560.phys.kobe-u.ac.jp

1 Introduction

The basic procedure in the renormalization group (RG) is to keep relevant information of a physical system, and neglect (or integrate out) irrelevant one. [1, 2, 3] The density matrix renormalization group (DMRG) introduced by White [4] greatly enhances the applicability of the numerical RG, because the method automatically keeps a fixed numbers ($= m$) of the relevant basis; DMRG present the best approximation within the limited numerical resource that we can use. The DMRG has been applied to a number of one-dimensional (1D) quantum lattice systems, such as the spin chain, [5, 6] ladder, [7, 8] Bethe lattice system, [9] strongly correlated electron systems, [11, 12, 13, 14] models in momentum space. [10] Not only the numerical superiority, but also the formulation of DMRG have attracted theoretical interests. Östlund and Rommer [15] have shown that DMRG is a variational method, where the ground state is expressed as a product of 3-index tensors. [16, 17] Martìn-Delgado and Sierra have investigated the analytic formulation of DMRG, and have formulated the correlated block RG. [18, 19] Recently White have refined the finite system algorithm of DMRG, and extend the applicability of DMRG to 2D quantum systems. [20] Quite recently Xiang have reported DMRG study of 1D quantum system at finite temperature, [21] using the quantum transfer matrix formulation [22] and DMRG applied to the transfer matrix. [23]

Another RG approach has been development for 2D classical lattice models: Baxter's method of the corner transfer matrix. (CTM) [24] The method is a generalization of Kramers-Wannier approximation, [25, 26] and therefore Baxter's method is based on a variational principle for the partition function. It should be noted that Baxter's variational relation is in principle the same as the variational relation in DMRG. [27] The purpose of this report is to explain

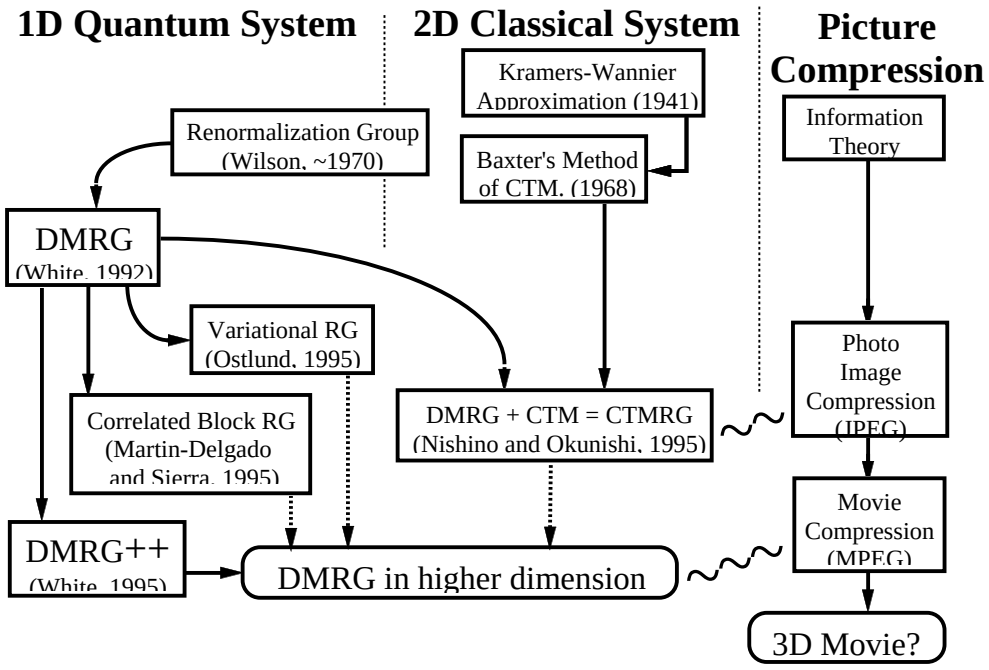

Figure 1: Historical overview of DMRG and related fields.

how the concept of DMRG is applied to 2D classical lattice models. We start from a short review of the variational relation in DMRG in the next section.

It is worth looking at a practical use of the RG method as the 2D photo image compression. [28, 29] A photo image in our computer is normally compressed before it is stored, in order to decrease the file size. The compression algorithm is related to the block RG method, [1, 3] since a small region — a pixel — in a 2D picture has strong correlation with its environment. (Computer scientists may insist that their findings about the photo image compression are efficient for RG formulation in physics.) At present, compression of movies — TV pictures — are in progress in the world of computation; [30, 31] the algorithm may be a good reference for the RG study of 3D classical systems and 2D quantum systems.

The development of RG, DMRG, Baxter's CTM method, and the photo image compression is summarized in Fig.1. Originally these methods are pro-

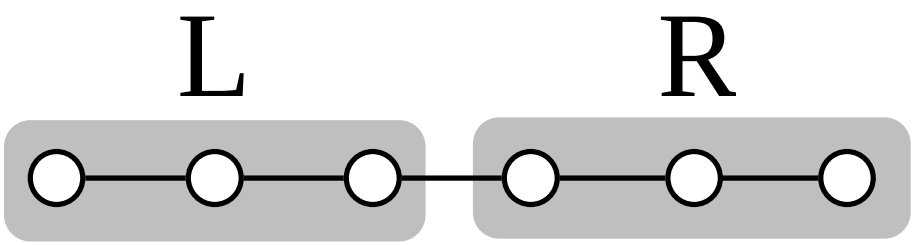

Figure 2: The $S = 1/2$ Heisenberg spin chain with open boundary conditions. We divide it into the local system $[L]$ and the reserver $[R]$.

posed independently, however, now it is apparent that their background is in common. It is, to approximate a system (or the *objects*) within a limited number of freedom.

2 Variational Principle in DMRG

We start from a short review of the variational principle in DMRG. We consider the antiferromagnetic $S = 1/2$ Heisenberg spin chain as an example of 1D quantum systems. The spin Hamiltonian is

$$H = J \sum_i \mathbf{S}_i \cdot \mathbf{S}_{i+1}, \tag{1}$$

where $\mathbf{S}_i$ represents the quantum spin at i-site, and the parameter J is positive. The Hamiltonian H is real-symmetric, and so is the density matrix $\rho = e^{-\beta H}$. (In the following discussion, ρ does not always have to be real-symmetric, but should be positive definite.)

We consider an open spin chain, (Fig.2) which consists of the left half $[L]$ (= the local system) and the right half $[R]$ (= the reserver). The terms 'local system' and 'reserver' are rather formal, since $[R]$ is not always longer than $[L]$. (In Fig.2 both $[L]$ and $[R]$ has the same size.) The Hilbert space of the whole system is spanned by the real-space basis $|\, l\,\rangle|\, r\rangle$, where $|\, l\,\rangle$ and $|\, r\rangle$ corresponds to the spin configuration for $[L]$ and $[R]$, respectively. The matrix

element of ρ is given by

$$\rho_{lr,l'r'} = \langle\, l\,|\langle\, r|e^{-\beta H}|\, r'\rangle|\, l'\,\rangle. \tag{2}$$

In the context of DMRG, what is called the *density matrix* is actually the density submatrix (DSM)

$$\rho^L = \sum_{ll'} |\, l\,\rangle\, \rho^L_{ll'}\, \langle\, l'\,| \;\equiv\; \sum_{ll'} |\, l\,\rangle \Big(\sum_r \rho_{lr,l'r} \Big) \langle\, l'\,| \tag{3}$$

that contains the information only about the local system $[L]$. The trace of ρ^L is equal to the partition function.

The relevant state selection — renormalization — in DMRG is performed through the diagonalization of the DSM

$$O^T \rho^L\, Q = \mathrm{diag}\{\lambda_1, \lambda_2, \ldots\}, \tag{4}$$

where $\lambda_1 \geq \lambda_2 \geq \ldots \geq 0$ are eigenvalues in decreasing order, $Q = (\mathbf{q_1}, \mathbf{q_2}, \ldots)$ are the set of the corresponding right eigenvectors, $O = (\mathbf{o_1}, \mathbf{o_2}, \ldots)$ are that of the left eigenvectors. The matrices O and Q satisfies the dual orthogonal relation $QO^T = 1$. When ρ^L is real-symmetric, Q is equal to O, and both of them are orthogonal matrices. The first m column vectors $\mathbf{q}_\alpha$ $(1 \leq \alpha \leq m)$ in Q represent the RG transformation from the original basis $\{|\, l\,\rangle|\, r\rangle\}$ to the renormalized basis $\{|\, \alpha\,\rangle\}$. The irrelevant states are thrown away. [4]

We can check the validity of the above basis state selection by observing the inequality

$$Z = \sum_l \lambda_l \;\geq\; \sum_{l=1}^{m} \lambda_l. \tag{5}$$

The quantity $\tilde{Z} = \sum_{l=1}^{m} \lambda_l$ is the approximate partition function, which is smaller than Z by $\sum_{l>m} \lambda_l$. It has been known that if the system has a finite excitation gap, the eigenvalue λ_i decays exponentially with respect to i, and therefore $\tilde{Z}$ is a good approximation for Z when m is sufficiently large.

The approximate partition function is equal to the trace of the m-dimensional diagonal matrix

$$\tilde{\rho}^L \equiv \mathrm{diag}\{\lambda_1, \lambda_2, \ldots, \lambda_m\} = \tilde{O}^T \rho^L \tilde{Q}, \tag{6}$$

where $\tilde{Q}$ is the rectangular matrix $(\mathbf{q_1}, \mathbf{q_2}, \ldots, \mathbf{q_m})$, and $\tilde{O}$ is $(\mathbf{o_1}, \mathbf{o_2}, \ldots, \mathbf{o_m})$. We can regard the matrix operation of $\tilde{O}^T$ and $\tilde{Q}$ to ρ^L as the RG transformation (or the block spin transformation), and $\tilde{\rho}^L$ as the renormalized DSM.

Substituting Eq.(6) into Eq.(5), we obtain a variational relation in the matrix form

$$Z = \mathrm{Tr}\, \rho^L \geq \mathrm{Tr}\, \tilde{\rho}^L = \mathrm{Tr}\, (\tilde{Q}\tilde{O}^T \rho^L), \tag{7}$$

where the matrix product $\tilde{1} \equiv \tilde{Q}\tilde{O}^T$ has the property of the projection operator $(\tilde{Q}\tilde{O}^T)^2 = \tilde{Q}\tilde{O}^T$. The projection operator $\tilde{Q}\tilde{O}^T$ is *optimal* in the sense that it gives maximum of $\tilde{Z} = \mathrm{Tr}\, (\tilde{1}\rho)$ under the constraint $\tilde{1}^2 = \tilde{1}$ and $\mathrm{Tr}\, \tilde{1} = m$. In other word, the DMRG minimize the free energy of the system within the restricted degree of freedom. At the zero temperature ($\beta \to \infty$), DMRG minimize the total energy.

The optimal projection operator $\tilde{1}$ for the local system $[L]$ is dependent on the size of the reserver $[R]$. However, the dependence is not conspicuous when $[R]$ is sufficiently large. The infinite system DMRG algorithm uses the insensitivity of $\tilde{1}$ against the reserver size. The finite system DMRG algorithm is more accurate than the infinite algorithm, because the former correctly takes into account of the reserver-size dependence.

3 From Quantum system to Classical system

In order to apply the variational relation in DMRG to 2D classical lattice system, we define the DSM for 2D systems. We use the fact that the density matrix $e^{-\beta H}$ of a d-dimensional quantum system can be expressed as a par-

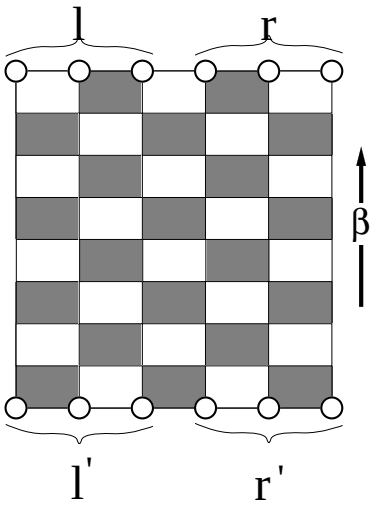

Figure 3: Trotter-Suzuki decomposition of the density matrix in Eq.(8). The label l, r, l' and r' denote the boundary spin configurations.

tition function of a d+1-dimensional classical system with special boundary conditions; the relation is known as the Trotter-Suzuki formula. [32, 33]

The density matrix of the Heisenberg chain in Fig.2 is approximated as

$$e^{-\beta H} = \left(e^{-\frac{\beta}{N}H}\right)^M \sim \left(e^{-\frac{\beta}{N}H_A}e^{-\frac{\beta}{N}H_B}\right)^M \tag{8}$$

where $H_A \equiv \sum_i \mathbf{S}_{2i} \cdot \mathbf{S}_{2i+1}$ and $H_B \equiv \sum_i \mathbf{S}_{2i+1} \cdot \mathbf{S}_{2i+2}$ are the partition of H. The matrix element $\rho_{lr,l'r'}$ in Eq.(2) is approximated by the Boltzmann weight of the *chessboard model*, whose boundary spin configurations are fixed to l, r, l' and r'. Figure 3 shows an example when $M = 4$. When we consider the partition function Z, the boundaries l, r, l' and r' plays the role of the tabs for sticking; $Z = \mathrm{Tr}\, e^{-\beta H}$ is approximately equal to the partition function of the cylindrical system shown in Fig.4(a), which is constructed by attaching l and r in Fig.3 to l' and r', respectively. In the same way, the approximate DSM $\rho^L_{ll'} = \sum_r \rho_{lr,l'r}$ is obtained by attaching r to r' as shown in Fig.4(b).

The expression of ρ^L in Fig.4(b) is a typical example of the DSM for 2D classical lattice models. The ρ^L corresponds to the cylindrical system with a

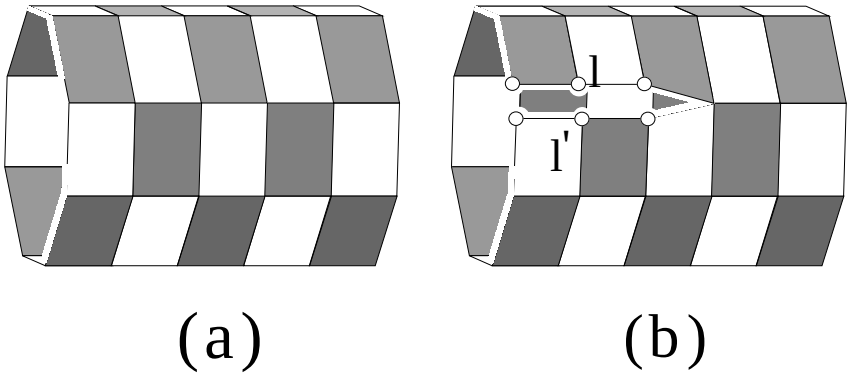

Figure 4: The density matrix in the Trotter-Suzuki formula Eq.(8): (a) partition function $\mathrm{Tr}\,\rho$. (b) density sub matrix $\rho^L_{ll'}$.

cut L, where the spin configurations around the cut are fixed to l and l'. We generalize this example. Suppose we have a finite size lattice system $[A]$ shown in Fig.5. We then consider an arbitrary line or curve L on $[A]$, and cut $[A]$ along L to derive a new system $[A']$. (The curve L is a kind of string on the 1+1 space time.) The derived system $[A']$ has new boundaries around the cut L, where the boundary spin configurations are represented by the labels l and l'. *The Boltzmann weight of* $[A']$, *which we write* $\rho^L_{ll'}$, *is the DSM of* $[A]$.

We have defined ρ^L for 2D classical lattice models. Once we obtain ρ^L for a given system $[A]$, we can perform DMRG along the variational treatment discussed in the previous section, where the group of spins l and l' on $[A]$ are transformed into m-state effective spins. In the next section we present an appropriate choice of $[A]$ and L for a typical 2D classical model.

4 Construction of the Density Matrix via CTM

The Trotter-Suzuki decomposed Heisenberg spin chain in Eq.(8) is an anisotropic 2D lattice model, and the application of DMRG on this system is rather

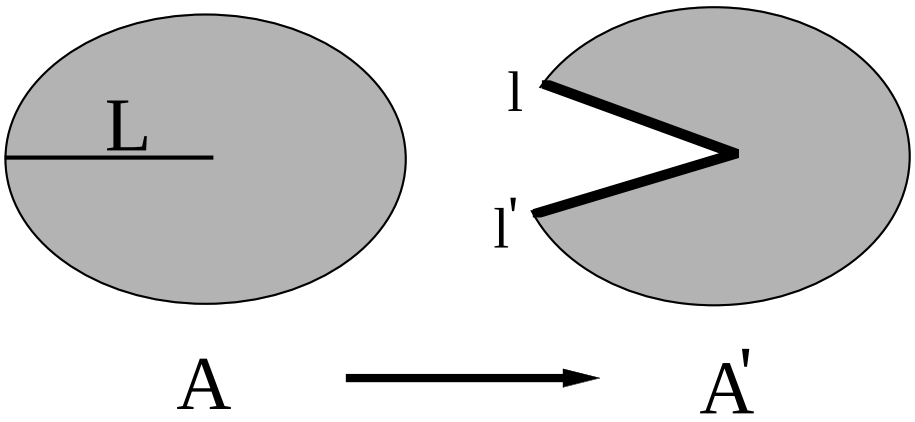

Figure 5: We derive the DSM of the finite size system $[A]$ by cutting it along the curve L. Compared to $[A]$, the system $[A']$ has additional boundaries l and l'.

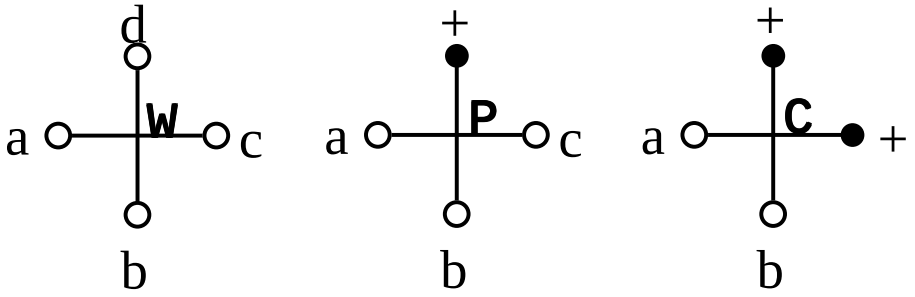

Figure 6: Boltzmann weights of the symmetric 16-vertex model; P and C are the boundary weights in Eq.(10) and Eq.(11), respectively.

complicated.[21] For the tutorial purpose we consider a simpler 2D system, the symmetric 16-vertex model. [24, 34] The model includes the Ising model [35] as its special case. For simplicity, we assume that the model is ferromagnetic.

The 16-vertex model is defined by the Boltzmann weight

$$W_{abcd} = W_{bcda} = W_{cdab} = W_{dabc} \tag{9}$$

on each vertex (= lattice point) of the simple square lattice, where the spin variables a, b, c, and d take either $+$ (up) or $-$ (down). In the following we consider a square system $[A]$, whose linear dimension is $2N$ or $2N + 1$. We

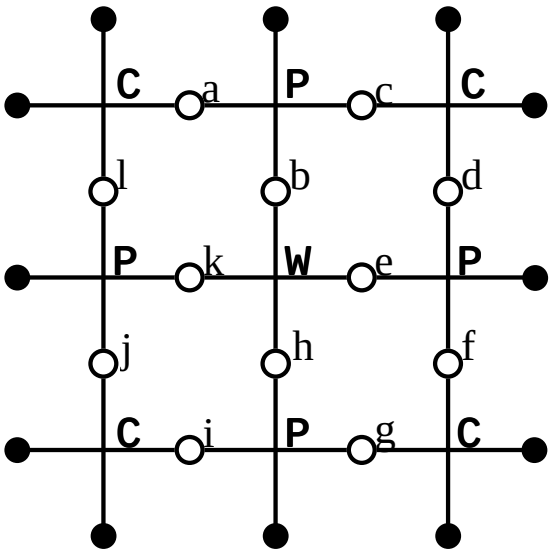

Figure 7: A square system of the linear dimension $2N+1=3$, whose partition function is given by Eq.(12).

impose fixed boundary condition on $[A]$; we introduce boundary weights

$$P_{abc} = W_{abc+} \tag{10}$$

and

$$C_{ab} = W_{ab++} \tag{11}$$

in order to fix the boundary spins to $+$. (Fig.6) The partition function of $[A]$ is expressed by these weights. For example, the partition function of the system with $2N+1=3$ is expressed as

$$Z = \sum_{ab\ldots l} W_{kheb} P_{abc} C_{cd} P_{def} C_{fg} P_{ghi} C_{ij} P_{jkl} C_{la}, \tag{12}$$

where the position of spin indices a-d is shown in Fig.7.

In order to generalize Eq.(12) to arbitrary system size, we introduce a half-row transfer matrix, (HRTM) which is a generalization of the boundary weight P in Eq.(10). The HRTM of length N is defined by the recursion relation

$$P^N_{\mathbf{a}b\mathbf{c}} = \sum_d W_{a_N\, d\, c_N\, b}\, P^{N-1}_{\mathbf{a}'d\mathbf{c}'}, \tag{13}$$

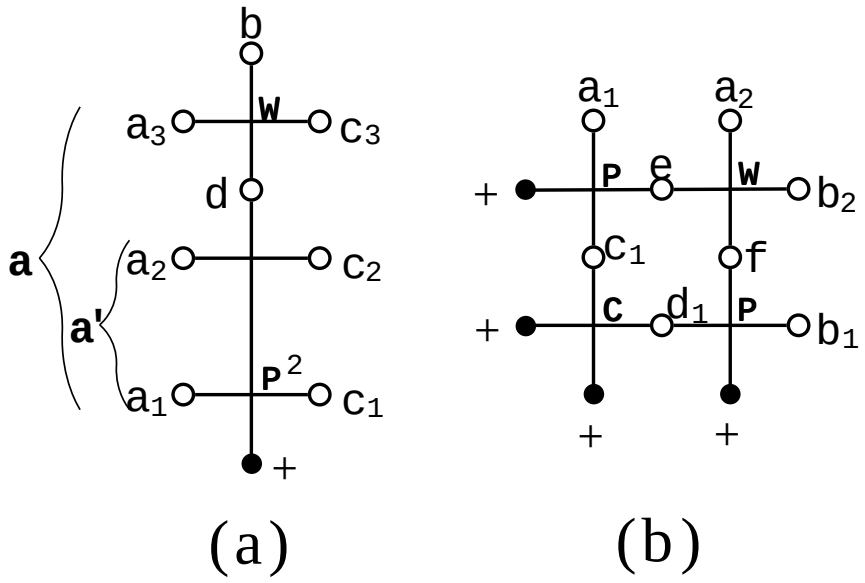

Figure 8: Recursive definition of (a) P^N in Eq.(13) and (b) C^N in Eq.(15). The shown examples are P^3 and C^2.

where the label N is the number of vertices in HRTM, $P^1_{\mathbf{a}b\mathbf{c}}$ is equal to P_{abc} in Eq.(10), and $\mathbf{a}$ represents a group of spins on a row

$$\mathbf{a} = (a_1, a_2, \ldots, a_{N-1}, a_N), \tag{14}$$

which is related to $\mathbf{a}'$ as $\mathbf{a} = (\mathbf{a}', a_N)$; the same for $\mathbf{c} = (\mathbf{c}', c_N)$. Figure 8(a) shows an example when $N = 3$. We occasionally drop the vector indices of $P^N_{\mathbf{a}b\mathbf{c}}$ and write it simply as P^N_b; in that case we think of P^N_b as a 2^N-dimensional matrix $(P^N_b)_{\mathbf{ac}}$. The HRTM is also conventionally called *vertex operator*. [36]

The density submatrix ρ^L of the square system $[A]$ is expressed as a product of corner transfer matrices. (CTMs) [24] The CTM of size N is defined as

$$C^N_{\mathbf{ab}} = \sum_{\mathbf{c}'\mathbf{d}'} \Big(\sum_{ef} W_{e\,f\,b_N\,a_N}\, P^{N-1}_{\mathbf{a}'e\,\mathbf{c}'}\, P^{N-1}_{\mathbf{b}'f\,\mathbf{d}'} \Big) C^{N-1}_{\mathbf{c}'\mathbf{d}'} \tag{15}$$

where we have used the index rule $\mathbf{a} = (\mathbf{a}', a_N)$, $\mathbf{b} = (\mathbf{b}', b_N)$, etc. Figure 8(b) shows the example when $N = 2$. The smallest CTM $C^1_{\mathbf{ab}}$ is equal to the boundary weight C_{ab} in Eq.(11). The square system $[A]$ is then constructed

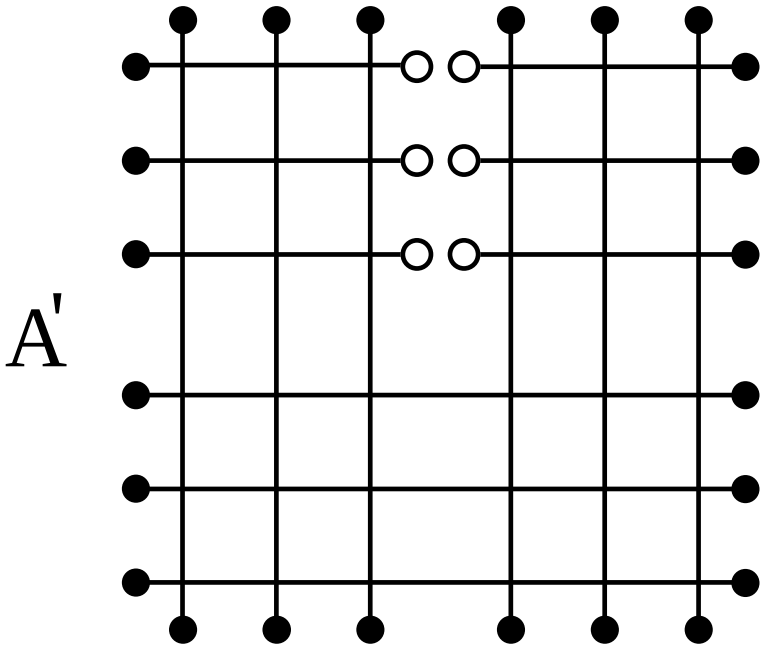

Figure 9: The density submatrix ρ^L of the square system $[A]$ is expressed as a product of four CTMs. (Eq.(16).)

by attaching four CTMs. Figure 9 shows the system $[A']$ of the size $2N = 6$, whose Boltzmann weight

$$\rho^L = (C^N)^4 \tag{16}$$

corresponds to the DSM of the square system $[A]$ of the size $2N = 6$. Such a construction of the DSM was first introduced by Baxter more than 30 years ago in his variational method. [24]

Now we can apply the RG procedure to 2D classical lattice models using ρ^L defined in Eq.(16); following the RG procedure in Sec.2, we combine Baxter's method and DMRG. For the brevity, we call our new RG method *corner transfer matrix renormalization group* (CTMRG) in the following. [27]

5 CTM Renormalization Group

As was discussed in Sec.2, the heart of DMRG is the diagonalization of ρ^L. For the symmetric 16-vertex model, where ρ^L is expressed as $(C^N)^4$, both ρ^L

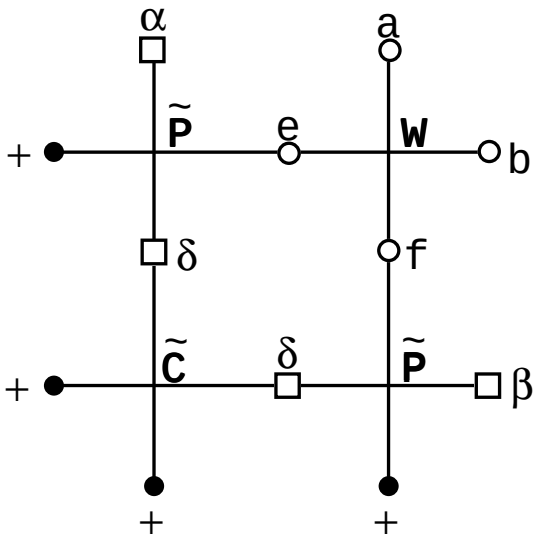

Figure 10: Area extension of the renormalized CTM in Eq.(20).

and C^N have the common eigenvectors. We therefore diagonalize CTM

$$O^T C^N Q = \mathrm{diag}\{\omega_1, \omega_2, \ldots\} \tag{17}$$

instead of ρ^L, where we assume the decreasing order $|\omega_1| \geq |\omega_2|, \ldots \geq 0$. The block-spin transformation is performed by the rectangular matrices $\tilde{O} = (\mathbf{o}_1, \mathbf{o}_2, \ldots, \mathbf{o}_m)$ and $\tilde{Q} = (\mathbf{q}_1, \mathbf{q}_2, \ldots, \mathbf{q}_m)$, where $\mathbf{o}_\alpha$ and $\mathbf{q}_\alpha$ are the left and the right eigenvectors of C^N, respectively. Here after we use greek letters for indices that runs from 1 to m. (Actually, $\tilde{Q}$ is equal to $\tilde{O}$ since C^N is symmetric.) The renormalized CTM

$$\tilde{C}^N \equiv \tilde{O}^T C^N \tilde{Q} = \mathrm{diag}\{\omega_1, \omega_2, \ldots, \omega_m\} \tag{18}$$

is related to $\tilde{\rho}^L \equiv \tilde{O}^T \rho^L \tilde{Q}$ via $\tilde{\rho}^L = (\tilde{C}^N)^4$. The renormalized HRTM is obtained in the same way

$$\tilde{P}_a^N = \tilde{O}^T P_a^N \tilde{Q}, \tag{19}$$

where the tensor elements of $\tilde{P}_a^N$ are $\tilde{P}^N_{\xi a \eta}$.

At this point we remember that P^N and C^N are defined through the recursion relations Eq.(13) and Eq.(15), respectively. The relations are also valid for

$\tilde{P}^N$ and $\tilde{C}^N$. For $\tilde{C}^N$, its area is extended by attaching two HRTMs (Fig.10)

$$\bar{C}^{\,N+1}_{(\alpha,a)(\beta,b)} = \sum_{ef\delta} W_{efba}\, \tilde{P}^N_{\alpha e\delta} \tilde{P}^N_{\beta f\delta}\, \omega_\delta, \tag{20}$$

where $\bar{C}^{\,N+1}_{(\alpha,a)(\beta,b)}$ is a *partially renormalized* CTM of linear size $N+1$, and the pairs of indices (α, a) and (β, b) represent the row and the column matrix indices for $\bar{C}^{N+1}$. The length of HRTM is simultaneously increased by putting a new vertex at the end point

$$\bar{P}^{N+1}_{(\alpha,a)b(\gamma,c)} = \sum_{d} W_{adcb} \tilde{P}^N_{\alpha d\gamma}\,. \tag{21}$$

The extended CTM in Eq.(20) is not diagonal. As was done in Eqs.(17-18), we diagonalize $\bar{C}^{N+1}$ to obtain the new renormalized CTM $\tilde{C}^{N+1}$ with the matrix dimension m. It is now obvious that we can indefinitely repeat the renormalization process in Eqs.(18-19) and the system size extension in Eqs.(20-21). In this way, we obtain $\tilde{P}^N$ and $\tilde{C}^N$ for arbitrary large N starting from P^1 and C^1. [27]

Approximate thermodynamic functions of $[A]$ can be obtained using $\tilde{C}^N$. The free energy $-k_BT \ln Z$ is estimated from the approximate partition function $\tilde{Z} = \mathrm{Tr}\,(\tilde{C}^N)^4 = \sum_i \omega_i^4$. It is also possible to obtain local quantities, such as spin polarization and multi-spin correlation functions, using a combination of P^N and C^N. For example, the local energy is estimated as

$$E(2N+1) = \frac{\sum_{abcd} X_{abcd} \mathrm{Tr}(\tilde{P}^N_a \tilde{C}^N \tilde{P}^N_b \tilde{C}^N \tilde{P}^N_c \tilde{C}^N \tilde{P}^N_d \tilde{C}^N)}{\sum_{abcd} W_{abcd} \mathrm{Tr}(\tilde{P}^N_a \tilde{C}^N \tilde{P}^N_b \tilde{C}^N \tilde{P}^N_c \tilde{C}^N \tilde{P}^N_d \tilde{C}^N)}, \tag{22}$$

where the position of the indices a-d are shown in Fig.11, and X_{abcd} is the local energy operator $\ln(W_{abcd})$. Since the CTMRG extends the area of the system $[A]$ from the center, local quantities at the center can be calculated most precisely.

The largest matrix element of $\tilde{C}^N$ rapidly grows with respect to N. We

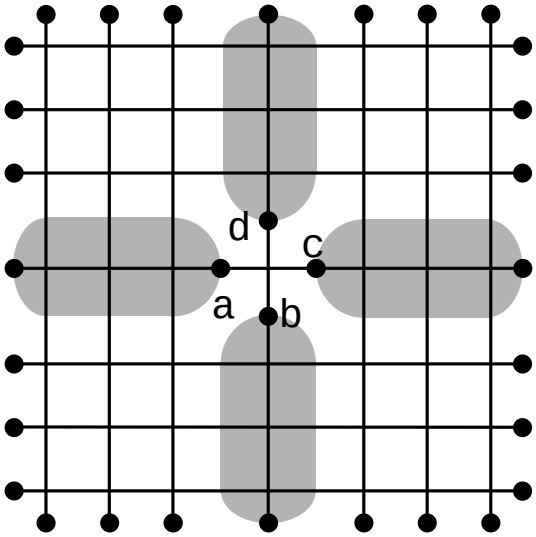

Figure 11: A square system of size $2N+1$ is expressed as a product among $\tilde{C}^N$, $\tilde{P}^N_{a\,(bcd)}$, and W.

should therefore normalize CTM

$$\frac{\tilde{C}^N}{\omega_1} = \mathrm{diag}\left\{1, \frac{\omega_2}{\omega_1}, \ldots, \frac{\omega_m}{\omega_1}\right\} \to \tilde{C}^N \tag{23}$$

in realistic numerical calculations. We should also normalize $\tilde{P}^N_a$ in the same manner. Apart from the critical point, the normalized $\tilde{C}^N$ converges to its thermodynamic limit $\tilde{C}^\infty$ exponentially with respect to N. At criticality the convergence is relatively slow; it is observed that the decay rate at criticality is controlled by the critical exponents. [37]

We have imposed fixed boundary conditions on $[A]$. Since the boundary condition is totally determined by the boundary weight P^1_a in Eq.(10) and C^1 in Eq.(11), we can choose other boundary conditions by modifying P^1_a and C^1. For example, the free boundary condition is imposed by the boundary weights

$$P_{abc} = W_{abc+} + W_{abc-} \tag{24}$$

and

$$C_{ab} = W_{ab++} + W_{ab+-} + W_{ab-+} + W_{ab--}. \tag{25}$$

The CTMRG method presented above can be applied to a wide class of 2D classical lattice models, such as the q-state Potts model, IRF model, etc. We have to be careful to anisotropic lattice models whose ρ^L consist of four *different* CTM's. (In Baxter's textbook the DSM are expressed as $\rho = ABCD$. [24]) In such a case, we should not diagonalize each CTM independently, but we should diagonalize ρ^L to perform RG transformation. We should also be careful to antiferromagnetic models, because we have to prepare several sets of $\tilde{P}^N$ and $\tilde{C}^N$ according to the alternating spin order.

6 Numerical Result

The symmetric 16-vertex model includes the square lattice Ising model as its parameter limit. We first look at the critical phenomena of the Ising model using CTMRG. Figure 12 shows the calculated local energy

$$E(2N) = \mathrm{Tr}\,(\sigma\sigma'\tilde{\rho}^L)/\tilde{Z} \tag{26}$$

where $\sigma\sigma'$ is a pair of neighboring spin at the center of the square cluster $[A]$ of size $2N$. The data shown by the black dots are $E(\infty)$, that are obtained when $m = 98$. The data deviate from the exact solution at most 10^{-7}. At the critical temperature T_c, we estimate $E_c(\infty)$ by observing its convergence with respect to N. The inset of Fig.11 shows the $1/N$ dependence of $E_c(N)$. A simple $1/N$ fitting gives $E_c(\infty) = 0.707148$, which is close to the exact one $1/\sqrt{2} = 0.707107\ldots$.

The $1/N$ dependence of $E_c(N)$ is actually related to the scale invariance at criticality. The finite size scaling (FSS) theory [38, 39] predicts that $E_c(N)$ obeys the scaling form

$$E_c(N) - E_c(\infty) \sim N^{1/\nu - d}, \tag{27}$$

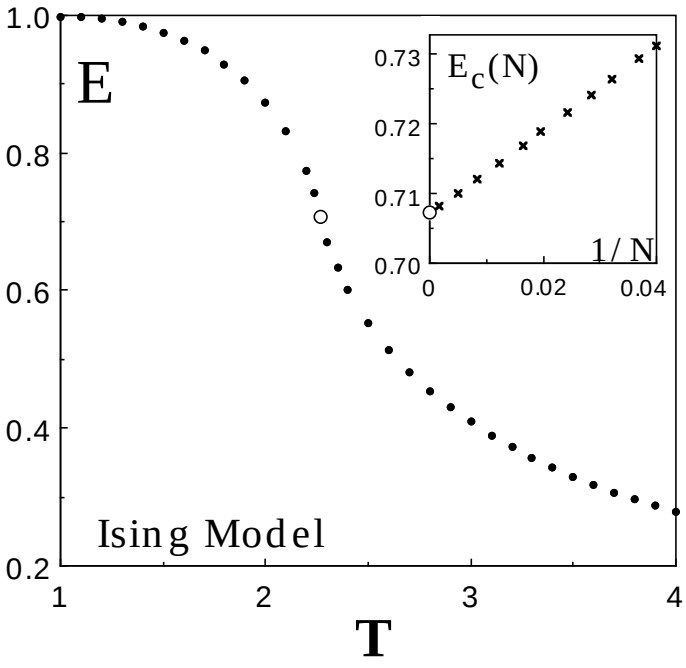

Figure 12: Local Energy $E(\infty)$ of the Ising Model at the center of the square system. The inset shows the size dependence of $E(N)$ at the critical temperature T_c.

where ν is the correlation-length exponent and $d = 2$ is the spatial dimensionality; in our case $E_c(N)$ is proportional to N^{-1} because ν of the Ising model is equal to unity. Similarly, the local order parameter

$$M(N) = \mathrm{Tr}\,(\sigma\tilde{\rho}^L)/\tilde{Z} \tag{28}$$

at the center of $[A]$ obeys

$$M_c(N) \sim N^{-(d-2+\eta)/2} \tag{29}$$

with the anomalous dimension of the spin η. Figure 13 shows the N dependence of calculated magnetization $M_c(N)$ at T_c when $m = 148$. As it is expected from $\eta = 1/4$, the calculated $M_c(N)$ is proportional to $N^{-1/8}$.

The estimation of the critical exponents via FSS is valid for a wide class of 2D classical model. As examples, we apply CTMRG and FSS to the q=2, 3 Potts models, [40, 41] which can be treated as a symmetric q^4-vertex model. [42,

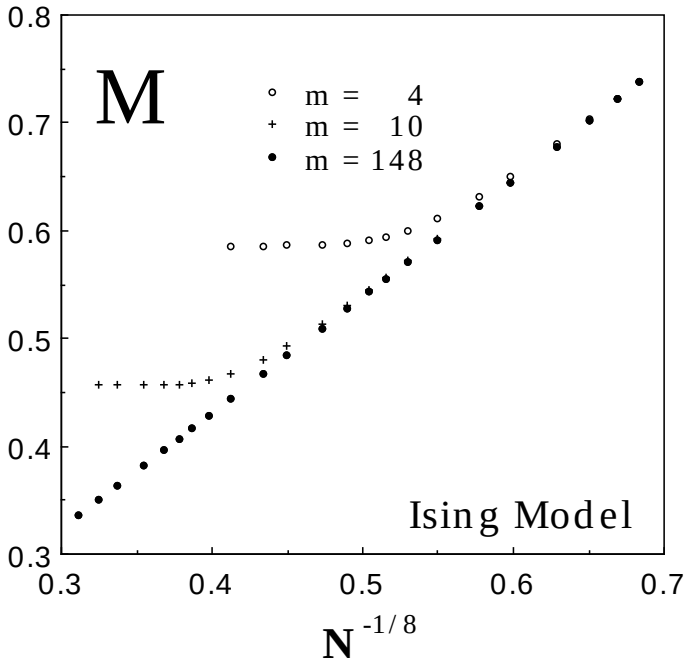

Figure 13: Local Magnetization of the Ising Model at T_c.

Table 1: Critical exponents ν and η of the q=2, 3 Potts model estimated from the numerical data when $m = 200$. Theoretical values are shown inside the parenthesis.

q	ν (Exact)	η (Exact)
2	1.0006 (1.0000)	0.2501 (0.2500)
3	0.8321 (0.8333)	0.2654 (0.2667)

41] Table I shows the estimated exponents ν and η from the calculated data when $m = 200$ and $100 \leq N \leq 1000$. For comparison, the theoretically determined exponents [41] are shown in the parenthesis. The error in the calculated exponents are less than 0.2%.

Numerical analysis of the case $q = 4$ is in progress. In this case, one has to take care of the logarithmic corrections in the FSS analysis. [43]

We finally show the N dependence of the local energy $E(N)$ of the q=5 Potts model at the transition temperature; we measure $E(N)$ from the average $E^* = (E_+ + E_-)/2$, where E_+ and E_- are the energy of the disordered and the ordered phase, respectively, at the transition temperature. (Fig.14) Since

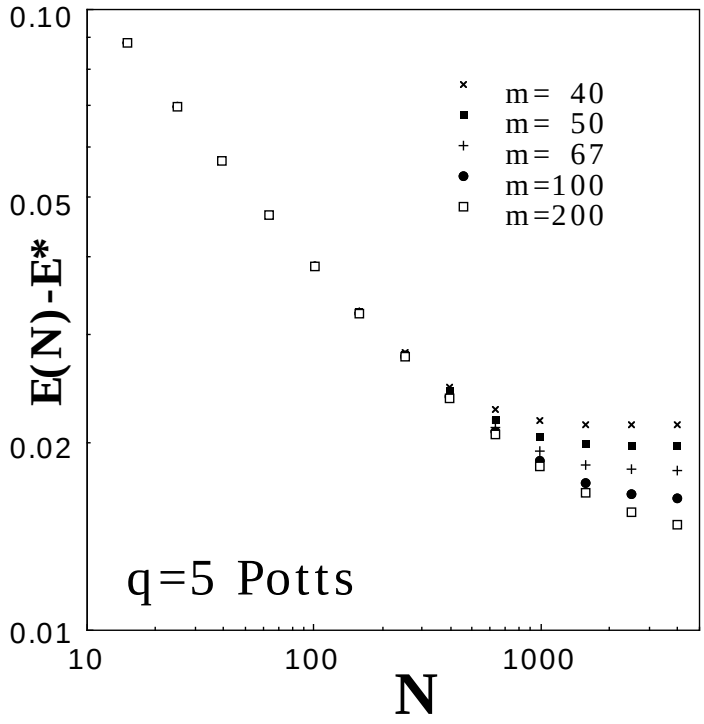

Figure 14: Local Energy of the q=5 Potts model.

the transition is first order, $E(N) - E^*$ does not obey the scaling form in Eq.(27). In this case, it is possible to estimate the latent heat through the scaling analyses with respect to both N and m. The calculated latent heat is 0.0256, where the exact value is 0.0265. [41] The CTMRG is expected to be efficient for the analysis of the weak first order transition. [44]

7 Conclusion and discussion

We have reviewed the variational principle in DMRG, and explained its application to 2D classical lattice systems. We create the DSM according to Baxter's construction, and perform the RG transformation using DMRG algorithm. As trial calculations, we perform FSS analyses on the q-state Potts models at the transition temperature. It is concluded that the CTMRG is efficient for the determination of the critical exponents or the latent heat.

It is possible to feed-back the CTMRG algorithm to the zero-temperature 1D quantum system, and to obtain a rapid infinite system DMRG algorithm; the product wave function (PWF) RG. [46] The PWFRG is closely related to the improved finite system DMRG algorithm (DMRG++ in Fig.1) recently proposed by White. [20]

Finally, we discuss the applicability of DMRG or CTMRG to 3D classical lattice models. As we have employed a square system for 2D models, we should consider a cubic system for 3D models. We divide it into 8 subcubics, say corner transfer tensor, (CTT) and construct the DSM as their tensor products. We then diagonalize the DSM, and renormalize CTT. Apart from the renormalized CTM in two dimension, renormalized CTT is not diagonal. [45] There is, however, a computational problem that prevents us from practical use of the RG method for 3D system; at present the numerical calculation is too heavy even for a small m.

There are plenty of subject that we can clarify in the field of the numerical RG.

Acknowledgments

The authors would like to express their sincere thanks to Y. Akutsu and M. Kikuchi for valuable discussions. T. N. thank to G. Sierra, M. A. Martìn-Delgado and S. R. White for helpful discussions about the RG method. The numerical result on $q = 5$ Potts model is obtained through the collaboration with A. Yamagata, H. Otsuka and Y. Kato. [44] The present work is partially supported by Kasuya foundation. Most of the numerical calculations were done by NEC SX-3/14R in computer center of Osaka University.

References

[1] L. P. Kadanoff: Physics 2 (1965) 263.

[2] K. G. Wilson and J. Kogut: Phys. Rep. **12 C** (1974) 75.

[3] T. W. Burkhardt and J. M. J. van Leeuwen: *Real-Space Renormalization,* Topics in Current Physics vol.**30**, (Springer, Berlin, 1982), and references therein.

[4] S. R. White: Phys. Rev. Lett. **69** (1992) 2863; Phys. Rev. **B 48** (1993) 10345; see also his article in this volume.

[5] S. R. White and D. A. Huse: Phys. Rev. **B48** 3844.

[6] E. S. Sorensen and I. Affleck: Phys. Rev. Lett **71** (1993) 1633; Phys. Rev. **B49** (1994) 15771.

[7] K. Hida: J. Phys. Soc. Jpn. **64** (1995) 4896.

[8] S. R. White and I. Affleck: to appear Phys. Rev. **B54** (1996).

[9] H. Otsuka: Phys. Rev. **B53** (1996) 14004.

[10] T. Xhiang: Phys. Rev. **53** (1996) R10445.

[11] C. C. Yu and S. R. White: Phys. Rev. Lett. **71** (1993) 3866.

[12] R. M. Noack, S. R. White and D. J. Scalapino: Phys. Rev. Lett **73** (1994) 882.

[13] N. Shibata, T. Nishino, K. Ueda and C. Ishii: Phys. Rev. **B53** (1996) R8828; preprint, cond-mat/9608118.

[14] S. R. White: preprint, cond-mat/9605143.

[15] S. Östlund and S. Rommer: Phys. Rev. Lett **75** (1995) 3537; preprint, cond-mat/9606213.

[16] A. Klümper, A. Schadschneider and J. Zittartz: Z. Phys. **B87** (1992) 281; Europhys. Lett. **24** (1993) 293.

[17] A. Schadschneider and J. Zittartz: Ann. Physik **4** (1995) 157.

[18] M. A. Martín-Delgado and G. Sierra: Int. J. Mod. Phys **A11** (1996) 3145; preprint, UCM/CSIC-96-01 July 1996; See also their article in this volume.

[19] M. A. Martín-Delgado, J. Rodriguez-Laguna and G. Sierra: Nuc. Phys. B473 (1996) 685.

[20] S. R. White: Preprint, cond-mat/9604129; see also his article in this volume.

[21] R. J. Bursill, T. Xiang, G. A. Gehring: preprint, cond-mat/9609001.

[22] M. Suzuki and M. Inoue: Prog. Theor. Phys. **78** (1987) 787.

[23] T. Nishino: J. Phys. Soc. Jpn. **64** (1995) 3598.

[24] R. J. Baxter: J. Math. Phys. **9** (1968) 650; J. Stat. Phys. **19** (1978) 461; *Exactly Solved Models in Statistical Mechanics* (Academic Press, London, 1982) p.363.

[25] H. A. Kramers and G. H. Wannier: Phys. Rev. **60** (1941) 263.

[26] R. Kikuchi: Phys. Rev. **81** (1951) 988.

[27] T. Nishino and K. Okunishi: J. Phys. Soc. Jpn. **65** (1996) 891-894.

[28] K. R. Rao and P. Yip: *Discrete Cosine Transform,* (Academic Press, INC, 1990.)

[29] M. Kaburagi, private communication.

[30] MPEG, CD 11172: *Coding of MovingPictures and AssociatedAudio for Digital Storage Media at Up To About 1.5 Mbps,* (1991).

[31] CCITT Rec. H.261, *Video Codec for Audiovisual Services at p*64 kbit/s,* CCITT COM XV-R 37-E (1990).

[32] H. F. Trotter: Proc. Am. Math. Soc. **10** (1959) 545.

[33] M. Suzuki: Prog. Theor. Phys. **56** (1976) 1454.

[34] M. Jimbo, T. Miwa and A. Nakayashiki: J. Phys. **26A** (1993) 2199.

[35] The origin of the Ising model is reported in S. Kobe, preprint cond-mat/9605174.

[36] T. Miwa, in *Correlation Effects in Low-dimensional Electron Systems,* Solid-State Science **118** ed. A. Okiji and N. Kawakami (Springer, Berlin, 1994) p.68.

[37] T. Nishino, K. Okunishi and M. Kikuchi: Phys. Lett. **A213** (1996) 69-72.

[38] M. E. Fisher, in *Proc. Int. School of Physics 'Enrico Fermi'*, edited by M.S. Green, (Academic Press, New York, 1971), Vol. 51, p. 1.

[39] M. N. Barber, in *Phase Transitions and Critical Phenomena*, edited by C. Domb and J.L. Lebowitz, (Academic Press, New York, 1983), Vol. 8, p. 146. and references therein.

[40] R. B. Potts: Proc. Camb. Phil. Soc. **48** 106.

[41] F. Y. Wu: Rev. Mod. Phys. **54** (1982) 235, and the references there in.

[42] T. Nishino and K. Okunishi: Preprint.

[43] J. Salas, A. D. Sokal: Preprint, lanhep-lat/9607030.

[44] T. Nishino, A Yamagata, H. Otsuka, Y. Kato and K. Okunishi: Preprint.

[45] Baxter: *Exactly Solved Models in Statistical Mechanics* (Academic Press, London, 1982) p.401.

[46] T. Nishino and K. Okunishi: J. Phys. Soc. Jpn. **64** (1995) 4084.